Energy Advances

ROYAL SOCIETY OF CHEMISTRY

PAPER

View Article Online
View Journal | View Issue

Cite this: *Energy Adv.*, 2024, 3, 1314

Performance evaluation of a newly developed transition metal-doped HZSM-5 zeolite catalyst for single-step conversion of C_1–C_3 alcohols to fuel-range hydrocarbons†

Ifeanyi Michael Smarte Anekwe, *[a] Bilainu Oboirien[b] and Yusuf Makarfi Isa[a]

This study investigated the performance of metal-doped HZSM-5 catalysts in the conversion of low alcohols to hydrocarbons (LATH). Catalysts, including unmodified HZSM-5 and metal-modified (Ni, Fe, and Co) HZSM-5, were evaluated at 350 and 400 °C with space velocities of 7 and 12 h^{-1} for LATH conversion. Characterisation techniques such as XRD, FTIR, SEM-EDS, PSD, N_2 adsorption, and TGA-DTA were employed. The characterisation results showed the successful metal incorporation in the HZSM-5 support catalyst. The overall evaluation of catalyst performance for LATH conversion revealed that the metal-doped catalysts showed a clear preference for liquid hydrocarbons with >99% average low alcohol conversion compared to the unmodified catalysts. In particular, Co/HZSM-5 and Fe/HZSM-5 showed a considerable preference for C_5–C_8 (62.81% and 54.95%), while Ni/HZSM-5 improved the synthesis of C_9–C_{12} (11.40%), C_{12}^+ (20.91%) and BTX (7.01%). The study on coke deposition indicated that Ni/HZSM-5 exhibited stability with minimal coke formation, while Co/HZSM-5 experienced higher coke deposition and deactivation tendencies in MTH and ETH conversions, respectively. Co/HZSM-5 exhibited the lowest weight loss, whereas Fe/HZSM-5 showed lower stability in PTH conversion. Notably, Ni/HZSM-5 demonstrated remarkable stability and performance in LATH conversion. These findings contribute to the advancement of catalysis and the transition towards a sustainable energy future.

Received 17th September 2023,
Accepted 19th May 2024

DOI: 10.1039/d3ya00460k

rsc.li/energy-advances

1. Introduction

In the 21st century, the world faces two critical challenges: the depletion of oil resources due to rising energy demands and the issue of global warming. It is widely recognised that the increased presence of carbon dioxide (CO_2) in the atmosphere is the primary driver of global warming. Recently, the urgency of addressing global warming has surged to the forefront of societal concerns, leading to heightened international awareness and a shared understanding of the need to reshape our society to tackle the root causes of CO_2 emissions and related pollution issues, including fine dust pollution.[1–3] Moreover, these challenges stem from our heavy reliance on fossil fuels as the primary energy source. While petroleum remains the most readily available fossil fuel for transportation, the current consumption rates project the depletion of oil reserves within the next 50 years, with natural gas reserves estimated to last approximately 70 years.[1] The discovery of new oil and gas reserves could delay the complete depletion of fossil fuels. However, it is crucial to recognise that significant fuel scarcity issues are anticipated in the future. Consequently, seeking an alternative sustainable energy source that can effectively address the challenges of projected energy scarcity and greenhouse gas emissions becomes imperative.

The C_1–C_3 alcohols, which are low alcohols (methanol, ethanol and propanol), have emerged as highly promising oxygenated fuels for decarbonising the road transport sector.[4,5] These alcohols offer several advantages, including a wide range of feedstocks and simplified production processes. In terms of fuel properties, low-carbon alcohols exhibit notable advantages over diesel and gasoline. These advantages encompass a high latent heat of vaporisation, lower adiabatic flame temperature, oxygenated molecular structure, absence of C–C bonds, higher oxygen content, lower viscosity, high H/C ratio, low sulfur content, and efficient evaporative cooling.[5,6] Despite its advantages, the lower calorific value of low alcohols compared to gasoline and their corrosiveness pose limitations on using 100% low alcohol in modern automobiles. As a result, the catalytic conversion of low alcohols using acid catalysts provides

[a] School of Chemical and Metallurgical Engineering, University of the Witwatersrand, Johannesburg 2050, South Africa.
E-mail: anekwesmarte@gmail.com
[b] Department of Chemical Engineering Technology, University of Johannesburg, Johannesburg, South Africa

† Electronic supplementary information (ESI) available. See DOI: https://doi.org/10.1039/d3ya00460k

a viable approach for upgrading them into fuel-range hydrocarbons (HCs). The conversion of low alcohols under optimal temperature conditions and in the presence of an acid catalyst such as ZSM-5 zeolite catalyst transforms low alcohol into intermediates and subsequently higher hydrocarbons (oligomers).[7] To enhance ZSM-5 catalyst performance, post-synthesis modifications are often employed. These modifications involve impregnation and ion exchange of zeolites with metal salts, phosphorus modification, alkali treatment, and steaming. They are claimed to improve hydrothermal stability, reduce deactivation, increase activity, or enhance selectivity towards specific product classes in the LATH process.[8] In addition, the choice of catalyst substitution method significantly impacts the catalyst's performance and lifespan.[9]

Since the introduction of Mobil's methanol-to-gasoline (MTG) process,[10] significant research has been dedicated to exploring the reaction and catalyst deactivation mechanisms involved in the transformation of alcohols for the production of liquid hydrocarbon fuels and light olefins using ZSM-5 zeolite as the catalyst.[11] ZSM-5 zeolites, which possess a uniform pore structure, high surface area, and adjustable acidity, have been extensively utilised in low alcohol-to-hydrocarbon (LATH) reactions, particularly methanol and ethanol. The LATH process typically involves a three-step approach before fractionation to meet fuel requirements, including alcohol dehydration, oligomerization, and hydrogenation. Alternatively, a one-step approach known as the consolidated alcohol dehydration and oligomerization (CADO) process has been proposed by Narula, Li.[12] It aims to achieve dehydration and oligomerization of alcohols in a single reactor. It has been observed that the dehydration of low alcohol typically occurs at temperatures below 300 °C,[13–19] and, in some cases, even lower than 200 °C.[13,20] Higher temperatures (>350 °C) promote secondary reactions of ethylene, such as oligomerisation and cracking, leading to the formation of longer-chain hydrocarbons, including gasoline-range HCs derived from light olefins.[7,21–23] Researchers have been exploring the potential of zeolites for the conversion of alcohols, with a particular focus on methanol and ethanol.[24] Tynjälä, Pakkanen[25] investigated the conversion of alcohols (C_1–C_4) at 370 °C using HZSM-5 (Si/Al = 54.4) and trimethyl-phosphite-modified ZSM-5 (Si/Al = 57), both exhibiting weak acidity. The conversion of low alcohols, such as methanol and ethanol, on trimethyl phosphite-treated ZSM-5 primarily produced ethers. However, due to the insufficient acidity of the weak acid sites, the further conversion of ethers into longer-chain HCs was not observed.[26]

For mesoporous materials, studies have shown that the Si/Al ratio (SAR) correlates with the catalytic performance and acidity of ZSM-5, which tends to decrease with increasing SAR.[2,27,28] Ramya, Sudhakar[28] observed a decrease in both percentage conversion and yield, which decreased from 70% for AlMCM-41/ZSM-5 (with Si/Al ratios of 25, 14, 10) to 28% at higher SAR values of 72 and 95. The percentage yield of gaseous products remained the same for all catalysts except those with SAR values of 72 and 95. The lower yield of gaseous products for zeolite catalysts with SAR values of 72 and 95 can be attributed to the lower Al content, which results in lower acidity.[28] Consequently, an increase in SAR for mesoporous materials improves the selectivity of liquid HCs, as lower acidity favours the formation of longer-chain HCs.[2,28] It has also been shown that metallic modifications facilitate secondary reactions and thus improve the yield of liquid HCs.[29] The study by Bi, Wang[30] on the conversion of methanol-to-hydrocarbon (MTH), showed that Zn-modified HZSM-5 (SAR of 38), improved aromatisation and liquid HC yield. However, the type of Zn species in the catalyst significantly altered the acidity of the catalyst surface, as coke deposition weakened olefin cyclisation in the early phase of the reaction. Over time, HC products, notably aromatics, present within zeolite pores undergo a series of reactions facilitated by the HC pool mechanism. These processes involve the methylation of aromatics formation of char and polyaromatic precursors such as coke. The accumulation of coke deposits within the zeolite pores leads to pore blockage, hindering the entry of reactants and products. Consequently, the acidic sites within the pores become inaccessible, resulting in decreased HC synthesis and catalyst stability during the reaction.[31]

While previous research into LATH conversion primarily focused on methanol and ethanol, often employing commercial ZSM-5 zeolite catalysts, there has been noticeably limited investigation into the conversion of propanol to fuel-range hydrocarbons using non-commercial catalysts. Specifically, the performance evaluation of newly synthesised transition metal-doped mesoporous ZSM-5 zeolite catalysts for C_1–C_3 alcohol conversion to fuel-range HCs remains unexplored. Based on an extensive literature review and to the best of our knowledge, this study represents a pioneering exploration of the catalytic potential of a newly developed metal-doped mesoporous ZSM-5 (Si/Al = 40) catalyst in the single-step conversion of C_1–C_3 alcohols into hydrocarbons. The study aims to fill this knowledge gap by investigating the relative performance of selected transition metal (Ni, Fe and Co) incorporation in a novel HZSM-5 catalyst for converting low alcohols into liquid (C_5^+) HCs. We also delve into understanding the mechanisms behind coke deposition, its correlation with catalyst properties, and the significant role of certain metals in inhibiting coke formation, which is essential for maintaining catalyst performance and longevity. As a result, these findings offer prospects for exploring new catalyst formulations, optimising operating conditions, and developing coke-resistant catalysts, thereby enhancing the efficiency of the LATH process.

2. Materials and methods

This study made use of the following chemicals: sodium silicate solution ((Na_2O)SiO_2·H_2O–), aluminium sulphate ($Al_2(SO_4)_3$·$18H_2O$), tetrapropyl ammonia bromide ($C_{12}H_{28}BrN$), sodium hydroxide (NaOH, 97%), sulfuric acid (H_2SO_4, 98% conc.), ammonium nitrate (NH_4NO_3). Nickel nitrate ($Ni(NO_3)_2$·$6H_2O$), iron nitrate ($Fe_2(NO_3)_2$·$18H_2O$), and cobalt nitrate ($Co(NO_3)_2$·$6H_2O$) are the precursors (99.9 wt% purity) that are used for transition metals. Methanol, propanol, and ethanol are the feedstocks. Sigma-Aldrich

supplied all chemicals. A hydrothermal reactor made of stainless steel and Teflon with a capacity of 200 mL was used to synthesise the catalyst.

2.1. Methods

The ZSM-5 catalyst support was prepared according to our previous work[32] using the hydrothermal catalyst synthesis technique, and the batch formula employed was $10Na_2O{:}40SiO_2{:}1.0Al_2O_3{:}10.5TPABr{:}3740{\cdot}6H_2O$. A silica source, 64.90 g of $(Na_2O)SiO_2{\cdot}H_2O$, and 1.82 g of NaOH were dissolved in deionised water to make the first solution. The second solution was created by dissolving 16.01 g tetrapropylammonium bromide in deionised water, and the third solution contained deionised water with 3.80 g aluminium sulfate dissolved in it. The solutions were stirred for 6 hours in the following order: solutions 1 and 2 were mixed and agitated constantly to hydrolyse the entire components. After stirring for one hour, solution 3 was added to the mixture, and the mixture was continued to be agitated rapidly for an additional five hours at a speed of 2000 revolutions per minute (RPM) until a homogeneous gel mixture was achieved. With the addition of sulfuric acid at a concentration of 98%, the initial pH of the gel was decreased from 11.53 to a stabilised pH of 10.73 (average). The solution was left undisturbed for 12 hours at room temperature before being transferred to a Teflon-lined stainless-steel reactor for hydrothermal crystallisation at a temperature of 180 °C for 24 hours. After the crystallisation phase, the solid product was allowed to cool to ambient temperature, recovered using filtration, and extensively washed with deionised water. The solid product was dried at 110 °C overnight and calcined at 550 °C for three hours to remove the organic template and produce Na-ZSM-5. Ion exchange was carried out at 80 °C using a 1 M solution of NH_4NO_3 at 10 ml g^{-1} catalyst. The sample was filtered and washed with deionised H_2O and then dried overnight at 110 °C once the ion exchange process had been completed to obtain the NH_4^+/ZSM-5. The ion-exchange procedure was carried out and repeated twice. The recovered NH_4^+/ZSM-5 was calcined at 550 °C for six hours, which resulted in the breakdown of ammonium ions and the emergence of the hydrogen (protonated) form of ZSM-5 (HZSM-5). Transition metals were incorporated into the catalyst at concentrations of 0.5 wt% *via* the incipient impregnation method. The catalyst was then allowed to dry overnight before being calcined for six hours at 550 °C. The modified HZSM-5 was designated as M/HZSM-5, which stands for 0.5 wt% (Ni, Fe or Co)/HZSM-5. In this context, M refers to 0.5 wt% transition metal.

The catalytic performance of ZSM-5 catalysts doped with transition metals on converting low alcohols into hydrocarbons was assessed at temperatures of 350 and 400 °C and weight hourly space velocities (WHSV) of 7 and 12 h^{-1}. Both glass beads and glass wool (0.045 g) were used as structural support for the catalyst bed. Methanol, propanol, and ethanol were used as the feedstock in the reaction. After the catalyst was initially activated at a temperature of 400 °C, an HPLC pump fed the low alcohols into the fixed-bed reactor made of stainless steel with an internal diameter (ID) of 1.02 cm and a length of 64.52 cm. Product selectivity and conversion (X) were calculated based on the work done by Sun, Ma.[33]

2.2. Catalyst characterisation and product analysis

The crystallinity of pure and transition metal-doped ZSM-5 was examined using a Bunker D2 Phase Diffractometer that utilised Cu-K1 radiation operating at 40 kV and 30 mA and scanned at a rate of 2° per minute. The functional groups were detected using a PerkinElmer Fourier Transform-Attenuated Total Reflectance – Infrared Spectrometer Spectrum-2 within the 4000–400 cm^{-1} range. The surface area and porous properties of the ZSM-5 zeolites were determined using the N_2 adsorption–desorption analyser, and prior to the measurement, the zeolites were degassed by heating them to 400 °C for six hours. The Barrett, Joyner, and Halenda (BJH) model was used to obtain the pore size distributions. The samples' morphology was examined using scanning electron microscopy through a ZEISS Sigma 300 VP, while particle size distribution was determined using the Malvern instrument. Energy dispersive X-ray spectroscopy (Oxford Instruments X-act PentaFET Precision ESD) and X-ray fluorescence were used to determine the elemental composition of the transition metals in the catalyst. Trace (Co) and major elements were identified using a Philips PW2404 X-ray spectrometer with a Moviol solution binder and Norrish Fusion 1 method.

The thermogravimetric/differential thermal analysis (TGA/DTA) was performed with the assistance of a TA Instrument Q50 USA thermal analyser between temperatures of 30 and 800 °C at a rate of 15 °C per minute. The sample was heated in N_2 flow (50 mL min^{-1}) from 30–200 °C, then switched to air from 200–800 °C. A YL6500 gas chromatograph (GC) system equipped with a Flame Ionization Detector (FID) and a Capillary Column was used to analyse HCs. The column program consists of the following: the temperature of 40 °C was used to inject the sample, followed by heating the column at a rate of 3 °C per minute to reach 50 °C and then kept at that temperature for 3 minutes. The column was then heated at a rate of 2 °C per minute to 60 °C and maintained for a minute. Subsequently, it was heated at a rate of 5 °C per minute until it reached 200 °C and kept at that temperature for a minute. Finally, the column was heated to 315 °C at a rate of 15 °C per minute and maintained at that temperature for 5 minutes. The GC analysis findings were based on the distribution of peak areas. The results of the catalyst characterisation can be found in the ESI.†

3. Results and discussion

3.1. C_1–C_3 conversion over transition metal-doped catalysts

The result of the low alcohol (C_1–C_3) conversion over transition metal-doped catalysts is presented below. MTH, ETH and PTH conversion was conducted at 350 and 400 °C and WHSV of 7 and 12 h^{-1}.

3.1.1. Methanol-to-hydrocarbon (MTH) conversion over transition metal-doped HZSM-5. The MTH conversion was conducted under different operating conditions to investigate the influence of these parameters and transition metal doping on product selectivity and methanol conversion. At an operating condition of 350 °C and a WHSV of 7 h^{-1}, both unmodified

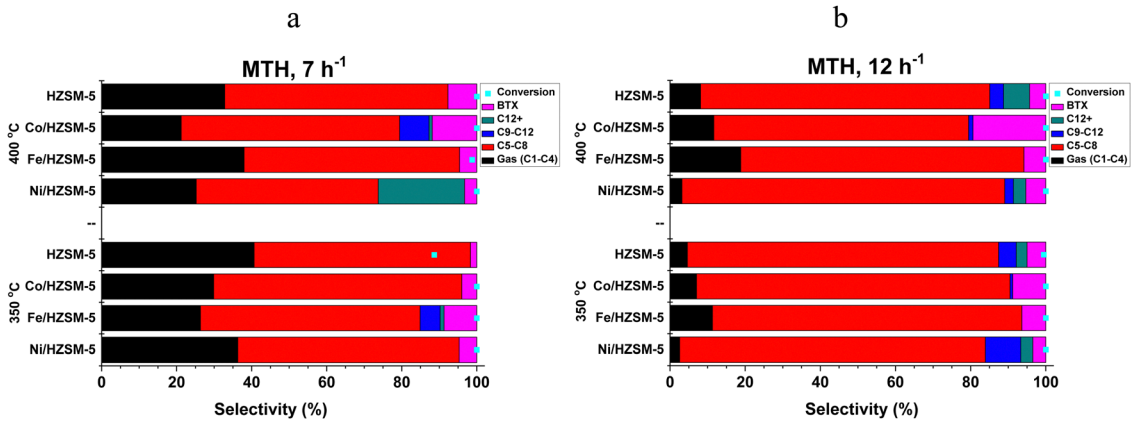

Fig. 1 (a) and (b) Product distribution and methanol conversion in the MTH process.

(HZSM-5) and metal-modified catalysts exhibited a preference for gaseous and C_5–C_8 hydrocarbons, with over 55% selectivity at this condition. However, the unmodified catalyst showed a significant selectivity towards C_1–C_4 hydrocarbons, reaching 40.61%. Transition metal doping improved methanol conversion and BTX (benzene, toluene, and xylene) selectivity, with the doped catalysts achieving 100% conversion compared to 88% for the unmodified catalyst (Fig. 1(a)). BTX selectivity also increased from 1.73% for HZSM-5 to 3.90%, 4.70%, and 8.71% with Co, Ni, and Fe-doped HZSM-5, respectively. Among the doped catalysts, Fe/HZSM-5 demonstrated a wider product distribution than others at this operating condition, with an appreciable preference for BTX and C_9–C_{12} HCs. When the temperature was increased to 400 °C while maintaining a WHSV of 7 h^{-1}, the unmodified HZSM-5 catalyst exhibited increased BTX selectivity by 6.01% and C_5–C_8 selectivity by 1.80%, resulting in a 7.8% decrease in the gaseous product compared to T = 350 °C, with a conversion of 100%. The modified catalysts showed similar selectivity towards C_5–C_8 hydrocarbons but declined gaseous HC selectivity. Co/HZSM-5 exhibited a wider product distribution, with appreciable selectivity towards C_9–C_{12} (7.89%) and BTX (11.91%) compared to other doped catalysts. Ni-doped catalysts favoured C_{12}^+ hydrocarbon production with 23% selectivity. Increasing the WHSV to 12 h^{-1} altered the product distribution, promoting the production of C_5–C_8 HCs (>81%) at 350 °C and (>67%) at 400 °C, with a significant decrease in gaseous products and >99% conversion for all catalysts tested (Fig. 1(b)). The reduction in C_5–C_8 HCs at 400 °C can be attributed to a shift in the reaction pathway with an increase in temperature promoting HC cracking and other secondary reactions that alter product selectivity. While Ni-doped and HZSM-5 catalysts showed selectivity towards a wide range of liquid HCs, Co and Fe-doped catalysts did not favour C_9–C_{12} and C_{12}^+ HCs at both investigated temperatures (350 and 400 °C) at WHSV 12 h^{-1}. Among the tested catalysts, Co-doped catalysts demonstrated the most significant selectivity towards BTX (19.41%) at a WHSV of 12 h^{-1} and 350 °C. Overall, the MTH process exhibited a preference for C_5–C_8 and BTX liquid hydrocarbon products over the tested catalysts.

3.1.2. Ethanol-to-hydrocarbon (ETH) conversion over transition metal-doped HZSM-5. The ETH conversion was investigated at similar operating conditions (WHSV = 7 and 12 h^{-1} and T = 350 and 400 °C). At a WHSV of 7 h^{-1}, the doped catalysts exhibited preference towards C_5–C_8, C_9–C_{12}, and BTX HC, while the unmodified catalysts favoured C_{12}^+ hydrocarbons at both temperatures. Among the metal-doped catalysts, Ni/HZSM-5 showed selectivity towards C_9–C_{12} (49.91%) and BTX (10.60%), whereas Co/HZSM-5 favoured C_5–C_8 HCs at 7 h^{-1} and 350 °C. The unmodified HZSM-5 catalyst exhibited the highest C_{12}^+ (65.81%) hydrocarbon selectivity, followed by Co/HZSM-5 (29.10%). Increasing the temperature to 400 °C at the same WHSV of 7 h^{-1} resulted in increased C_5–C_8 HC selectivity for all catalysts, accompanied by a decrease in gaseous products (C_1–C_4) and >99% ethanol conversion (Fig. 2(a)). Co/HZSM-5 and Fe/HZSM-5 catalysts showed increased C_5–C_8 selectivity by 15.62% and 25.8%, and BTX selectivity by 0.87% and 10.53%, respectively. Ni/HZSM-5 exhibited a 2.90% increase in C_9–C_{12} selectivity and a corresponding 2.1% decrease in C_{12}^+ selectivity, while HZSM-5 showed a 36.10% decrease in C_{12}^+ selectivity. Higher temperatures promoted rearrangement and cyclisation reactions, favouring the formation of higher-molecular-weight hydrocarbons. This can be attributed to the secondary reactions of reactive intermediates formed during ethanol conversion, leading to C_5^+ HCs through alkylation, cyclisation, and rearrangement reactions.[34] Increasing the WHSV to 12 h^{-1} resulted in reduced gaseous HCs (C_1–C_4), increased C_{12}^+ selectivity, and >98% ethanol conversion, indicating a shift towards liquid HC production at all temperatures investigated (Fig. 2(b)). This can be attributed to less contact time created by the increased WHSV promoting the production of liquid HCs while hindering HC cracking process. Metal-modified catalysts showed selectivity towards C_5–C_8, C_9–C_{12}, and BTX HCs, while the unmodified catalysts improved C_{12}^+ HCs at 7 h^{-1} and 350 °C. Among the catalysts, Ni/HZSM-5 exhibited the highest C_5–C_8 (48.4%) and BTX (5.0%) selectivity, and Fe/HZSM-5 enhanced C_9–C_{12} (37.0%). Similarly, HZSM-5 showed the highest C_{12}^+ selectivity (52.10%), followed by Co/HZSM-5 (40.11%) at 7 h^{-1} and 350 °C. Increasing the temperature to 400 °C at a WHSV of 12 h^{-1} resulted in a shift in product

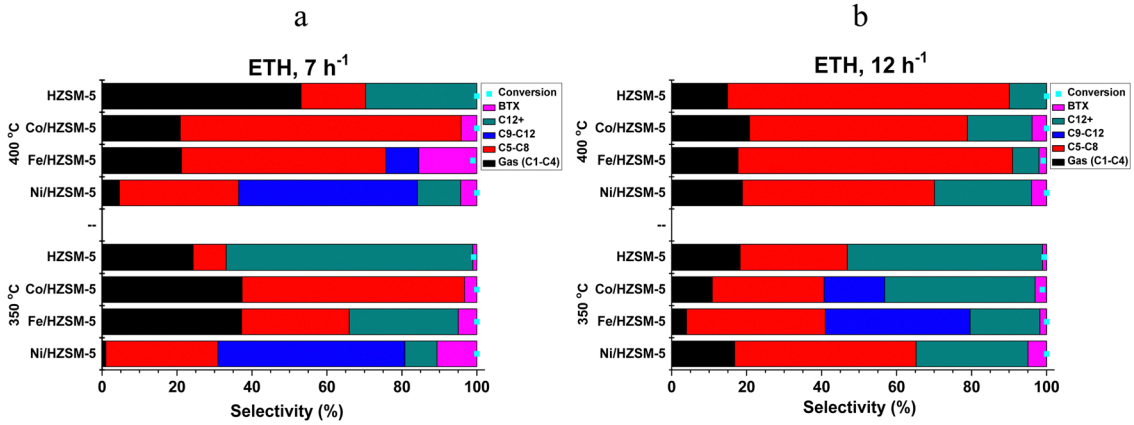

Fig. 2 (a) and (b) Product distribution and ethanol conversion in the ETH process.

distribution, with increased C_5–C_8 (51–75%) and BTX (>2%) selectivity compared to the operating temperature of 350 °C. However, C_9–C_{12} HCs were not favoured by all catalysts at this operating temperature, indicating the influence of reaction kinetics and catalyst properties on selectivity.

3.1.3. Propanol-to-hydrocarbon (PTH) conversion over transition metal-doped HZSM-5. The PTH conversion was investigated at WHSV of 7 and 12 h^{-1} and temperatures of 350 and 400 °C. At a WHSV of 7 h^{-1}, propanol conversion rates exceeding 96% were achieved, and all catalysts exhibited broad product distributions with significant selectivity towards gaseous products (C_1–C_4), C_5–C_8, and C_{12}^+, at both temperatures. Among the catalysts tested at a WHSV of 7 h^{-1} and a temperature of 350 °C, Ni/HZSM-5 exhibited the highest selectivity towards BTX (12.40%) and C_{12}^+ HCs (22.13%), while Fe/HZSM-5 favoured C_5–C_8 (53.10%) and C_9–C_{12} (6.30%). Co/HZSM-5 showed a preference for C_5–C_8 (43.9%) and C_{12}^+ (21.73%) HCs. Increasing the temperature to 400 °C at a WHSV of 7 h^{-1} resulted in a slight alteration in the product distribution. The metal-doped catalysts exhibited high selectivity towards specific HC fractions, particularly C_5–C_8 (34.1–57.4%) and BTX (2.61–19.40%). Co and Ni-doped catalysts displayed the highest selectivity towards these HC fractions. For Ni/HZSM-5, a decrease in the selectivity of C_1–C_4 and C_{12}^+ HCs led to a corresponding increase in C_5–C_8, C_9–C_{12}, and BTX by 12.50, 3.71, and 7.10%, respectively. Fe/HZSM-5 exhibited an increase of 9.0% in C_1–C_4, 9.6% in C_{12}^+, and 2.3% in BTX, with a decline of >1.50% in the selectivity of other HC fractions. Co/HZSM-5 recorded a 13.5% increase in C_5–C_8 selectivity, resulting in a decrease in the selectivity of other HC fractions. The unmodified catalyst showed a 1–6% increase in all HC fractions, except for C_5–C_8 HC, which experienced a 16.8% decrease in selectivity at 7 h^{-1} WHSV and temperature of 400 °C. At a WHSV of 12, the PTH conversion revealed a significant decline in gaseous HCs, leading to an increase in the selectivity of liquid HCs fraction (C_5^+) at all temperatures tested. Different catalysts exhibited the highest selectivity for various HC fractions: Ni/HZSM-5 achieved 89.81% selectivity for C_{12}^+, Co/HZSM-5 reached 88.6% selectivity for C_5–C_8, and Fe/HZSM-5 recorded selectivities of 22.01, 11.60, and 1.91% for C_9–C_{12}, C_1–C_4, and BTX HC fractions, respectively, at 12 h^{-1} and 350 °C. However, the unmodified catalyst exhibited a product distribution comparable to the metal-doped catalysts at this operating condition. At 400 °C and 12 h^{-1}, with a propanol conversion rate of >98%, a moderate change in the product distribution was observed, including a decline in gaseous products and an increase in BTX. Although a similar trend was observed at a WHSV of 7 h^{-1}, the changes varied across different HC fractions. Compared to the selectivity at 350 °C, the unmodified HZSM-5 catalysts showed a significant selectivity towards C_{12}^+ HCs (80.0%), decreasing the selectivity of other fractions. Ni/HZSM-5 promoted the selectivity of C_5–C_8, C_9–C_{12}, and BTX by 51.70, 6.61, and 10.80%, respectively, attributed to a significant decrease in C_{12}^+ selectivity. On the other hand, Fe and Co-doped HZSM-5 catalysts drastically increased the selectivity of C_5–C_8 and C_{12}^+ HCs by 16.6% and 8.30%, respectively. These findings demonstrate the influence of temperature, WHSV, and catalyst type on HC fractions' product distribution and selectivity in the PTH process (Fig. 3).

3.1.4. Comparative evaluation of catalyst performance in LATH conversion. Table 1 presents the average performance of various catalysts in the LATH conversion, while Fig. 4 illustrates their average conversion and phase selectivity of different low alcohols. All values reported in this comparative study are average values. In the MTH process, there is no significant change in selectivity towards C_5–C_8 and C_9–C_{12} HCs, with all catalysts recording an average selectivity of 68–69% and 1–3%, respectively. Ni-doped HZSM-5 exhibited the highest selectivity for C_{12}^+, while Co/HZSM-5 favours BTX among all the tested catalysts. The unmodified catalyst lags behind the modified catalysts by approximately 3% in methanol conversion. Additionally, compared to other catalysts, Ni and Co-doped HZSM-5 demonstrated slightly higher selectivity towards liquid HCs, with 83% and 82%, respectively. In the PTH process, the highest selectivity of 63.9% for C_5–C_8 is observed over Co/HZSM-5, Fe/HZSM-5 recorded a selectivity of 9.61% for C_9–C_{12}, Ni/HZSM-5 showed selectivity of 36.4% for C_{12}^+ and 10.72% for BTX. All catalysts exhibited similar propanol

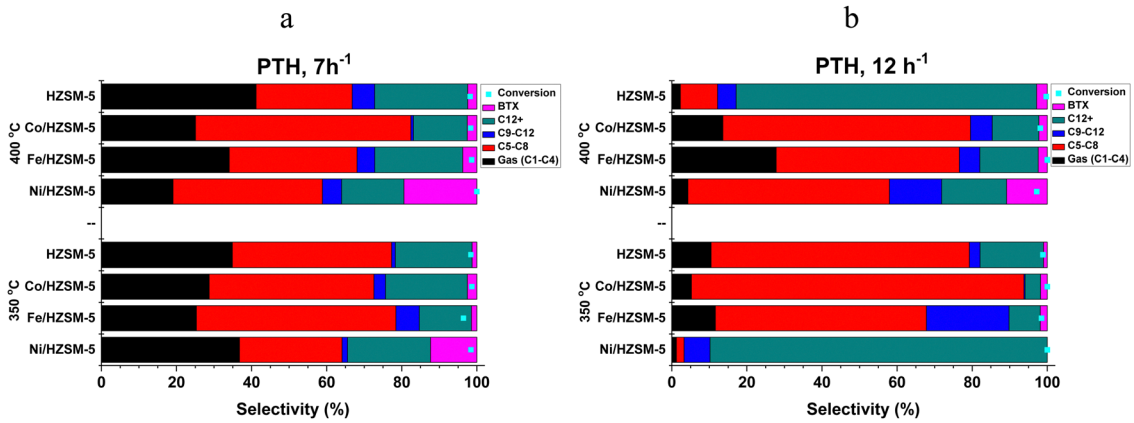

Fig. 3 (a) and (b) Product distribution and propanol conversion in the PTH process.

Table 1 Summary of (average) product selectivity and conversion (%) in LATH (C_1–C_3) conversion over metal-doped HZSM-5 catalysts

Catalysts	Gas (C_1–C_4)	C_5–C_8	C_9–C_{12}	C_{12}^+	BTX	Conversion	Liquid
MTH conversion							
ZSM-5	21.54	69.24	2.09	2.44	4.69	97.03	78.46
Ni/HZSM-5	16.80	68.70	2.94	7.36	4.19	100.00	83.20
Fe/HZSM-5	23.60	68.42	1.34	0.26	6.38	99.69	76.40
Co/HZSM-5	17.44	68.90	2.43	0.21	11.02	100.00	82.56
Average	19.85	68.81	2.20	2.57	6.57	99.18	80.15
ETH conversion							
ZSM-5	27.63	32.44	0.00	39.38	0.54	99.63	72.37
Ni/HZSM-5	10.32	40.35	24.41	18.94	5.99	100.00	89.68
Fe/HZSM-5	20.02	48.38	11.85	13.68	6.08	99.51	79.98
Co/HZSM-5	22.45	55.58	4.04	14.33	3.60	99.72	77.55
Average	20.11	44.19	10.08	21.58	4.05	99.72	79.89
PHT conversion							
ZSM-5	22.20	36.67	3.72	35.51	1.90	98.80	77.80
Ni/HZSM-5	15.35	30.70	6.84	36.45	10.66	98.90	84.65
Fe/HZSM-5	24.69	48.04	9.61	15.29	2.38	98.38	75.31
Co/HZSM-5	18.15	63.93	2.48	13.16	2.28	98.79	81.85
Average	20.10	44.84	5.66	25.10	4.30	98.72	79.90
(b) Catalyst preference for HC fractions in LATH (C_1–C_3) conversion: an average evaluation							
ZSM-5	23.79	46.12	1.94	25.78	2.38	98.49	76.21
Ni/HZSM-5	14.16	46.58	11.40	20.92	6.95	99.63	85.84
Fe/HZSM-5	22.77	54.95	7.60	9.74	4.95	99.19	77.23
Co/HZSM-5	19.35	62.80	2.98	9.23	5.63	99.50	80.65

conversion rates, averaging 98.71%. Similar to MTH, PTH also favours liquid HCs in terms of phase selectivity, with Ni and Co-doped HZSM-5 catalysts showing slightly higher selectivity compared to Fe/HZSM-5 and HZSM-5, which exhibited slightly higher selectivity towards gaseous HCs (C_1–C_4). Furthermore, in the ETH process, all tested catalysts achieved approximately 100% conversion, with similar phase selectivity except for Ni/HZSM-5, which recorded the highest selectivity of 89.7% towards liquid HCs. Ni/HZSM-5 and Co/HZSM-5 demonstrate the highest average selectivity for C_9–C_{12} and C_5–C_8 at 24.4 and 55.60%, while Fe/HZSM-5 and HZSM-5 promote the production of BTX (6.10%) and C_{12}^+ (39.41%) HCs respectively. Compared to methanol feedstock, the performance of ethanol in LATH conversion displays a strong correlation with propanol, as evidenced by their similar percentage selectivity to HC fractions, as shown in Table 1. While methanol feedstock exhibits greater selectivity towards C_5–C_8 and BTX, ethanol and propanol show a broader product distribution, favouring longer-chain HCs. This suggests that the feedstock type is another determining factor in altering the product distribution, in addition to the influence of different catalysts and operating parameters. The observed trend exhibited by different feedstocks may be attributed to several factors, including the molecular size of low alcohols, carbon chain length, and diffusion rates.

Methanol has the smallest molecular size; hence, higher adsorption uptake among the three low-alcohol feedstock investigated, followed by ethanol and propanol (kinetic diameter,

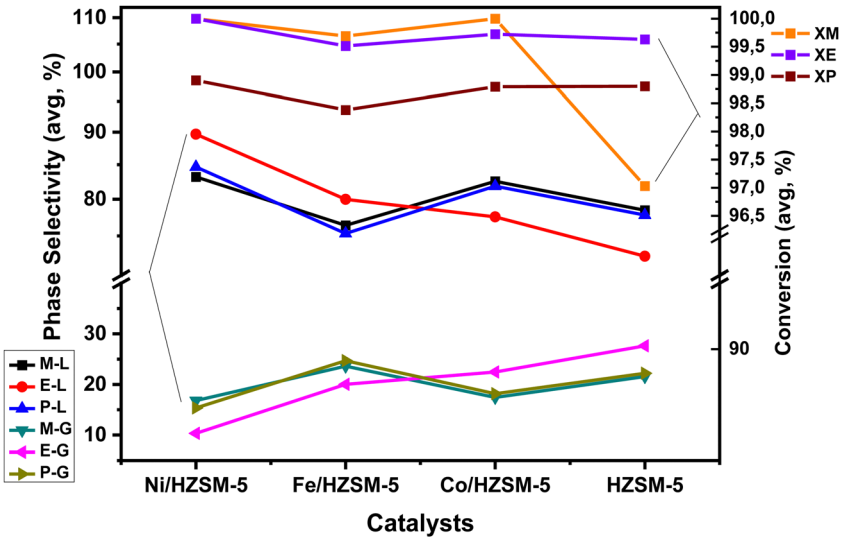

Fig. 4 Average phase selectivity and conversion in the LATH process over metal-doped catalysts (XM, XE, XP – MTH, ETH, & PTH conversion; M-L, E-L, P-L and M-G, E-G, P-G – liquid and gaseous HC products from MTH, ETH, & PTH).

3.6 Å ≪ 4.3 Å < 4.9 Å).[35,36] This size difference influences their behaviour within the 1D pores). The size of the alcohol molecule affects the reactivity and diffusion properties during catalytic conversion. Smaller molecules like methanol are generally more reactive than larger molecules like ethanol and propanol.[35,37] In addition, higher diffusion rates tend to favour the production of smaller chain hydrocarbons in low-alcohol conversion processes. Diffusion plays a crucial role in the reaction kinetics and mass transfer during the conversion of alcohols to hydrocarbons. When the diffusion rate is high, reactant molecules can more readily access the catalyst's active sites, leading to a higher frequency of collisions and a higher reaction rate. However, in the case of low alcohol conversion, higher diffusion rates also promote the rapid transport of intermediates and products away from the active sites, limiting their further reactions. With higher diffusion rates, the intermediates and products are more likely to diffuse away before undergoing further reactions, resulting in a greater proportion of smaller chain hydrocarbons in the case of methanol feedstock. On the other hand, slower diffusion rates can promote longer chain growth by allowing more time for the intermediates to interact with the catalyst and undergo subsequent reactions, such as oligomerisation and polymerisation, leading to the formation of larger hydrocarbon molecules as exhibited in ETH and PTH process. Furthermore, the carbon chain length and the functional group bound impact the low alcohol reactivity, product type and distribution. Methanol is one-carbon alcohol, ethanol is two-carbon alcohol, and propanol is three-carbon alcohol, all possessing different alkyl groups. The functional group attached to a methyl group experiences less steric hindrance than one attached to an ethyl or larger hydrocarbyl group.[37–39] Longer carbon chains tend to favour the production of higher molecular weight HCs in the case of ethanol and propanol. However, it's important to note that aside from low alcohol feedstock, specific conditions, such as catalyst type, temperature, and WHSV, also influence product distribution in low alcohol conversion processes. The impact of diffusion rates should be considered in conjunction with these factors to understand the overall outcome of the process. Table 1b presents the average catalyst preference for HC fractions in LATH conversion.

The conversion of low alcohols to hydrocarbons (LATH) has been extensively investigated using various catalysts, predominantly zeolites/modified zeolites.[16,40–43] Depending on the catalyst employed, different reaction mechanisms have been proposed. In the case of ZSM-5 zeolite catalysts, the mechanism of LATH is suggested to involve an intermediate species, with hydrocarbon production occurring through secondary reactions.[16,44] Specifically, for this study, we hypothesised that low alcohols initially undergo dehydration to form olefins, followed by the conversion of olefins into hydrocarbons (including C_3^+ olefins, BTX, and C_5^+) *via* acid-catalysed oligomerisation-cracking and oligomerisation-aromatisation mechanisms. Other studies have also reported similar pathways.[16,45] Generally, the mechanism of MTH consists of methanol dehydration and hydrocarbon production *via* the hydrocarbon pool mechanism. The MTH pathway is an autocatalytic process which proceeds through several steps. Initially, methanol molecules are adsorbed onto the acid sites of the ZSM-5 catalyst through hydrogen bonding and van der Waals interactions. Dehydration of the adsorbed methanol occurs, forming dimethyl ether (DME–CH_3OCH_3) as an intermediate. This intermediate, CH_3OCH_3, can undergo further reactions, including carbocation formation through proton transfer from the acid site to the methoxy group. Subsequently, alkyl migration within the zeolite channels or pores leads to structural rearrangements and the formation of different HC isomers, while oligomerisation and polymerisation reactions promote the growth of HC chains (C_5^+). Furthermore, other reactions, such as cracking and fragmentation, can break down larger HC molecules into smaller fragments, generating various HC products. Ultimately, the hydrocarbon products desorb from the catalyst surface,

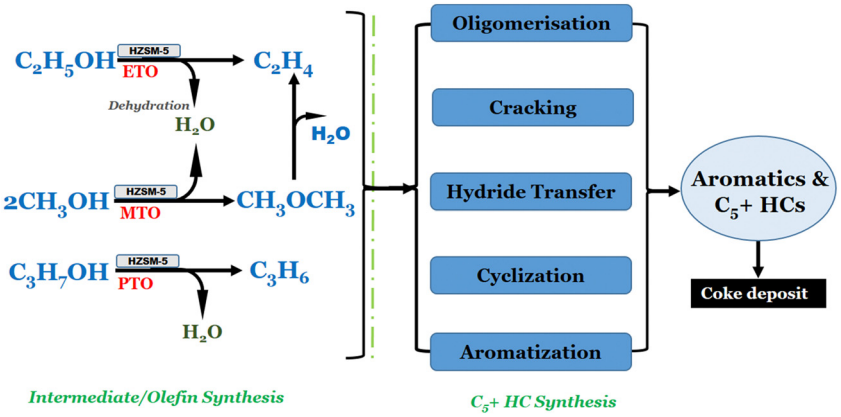

Fig. 5 Reaction pathway for the conversion of low alcohols (methanol, ethanol and propanol) to hydrocarbons.

providing the desired products of the MTH conversion process.[16,44,45]

It was believed that ethanol primarily undergoes intermolecular dehydration to form ethylene and diethyl ether (DEE) through a concerted mechanism.[46] DEE can undergo cracking to produce additional ethylene, providing an alternative reaction pathway (Fig. 5). The cracking of DEE occurs *via* acid-catalysed or radical mechanisms. Ethylene generated from dehydration and DEE cracking can undergo dehydrogenation to form ethyl radicals. These ethyl radicals from dehydrogenation react with adsorbed HC species on ZSM-5 catalyst, forming carbocations, which participate in secondary reactions such as aromatisation leading to aromatics (BTX) and long chain (C_5^+) HCs through oligomerisation.[16,46–48] Similar mechanisms apply to secondary and tertiary alcohols like isopropanol, where propene is an intermediate produced *via* dehydration. Propene can undergo further reactions to yield various hydrocarbon products.[49–51] The presence of metal species in the doped HZSM-5 catalysts promotes the initial dehydration of low alcohol to form an intermediate including olefins, followed by the oligomerisation and cracking of this intermediate to form a range of hydrocarbons and coke deposition. For this study, we believe that intermediate formation is favoured by the presence of Ni^{2+}, Co^{2+} or Fe^{3+} species, which act as active Lewis acid sites, promoting the dehydration of low alcohols.[16,44] However, the presence of Co^{2+} species on the catalyst surface can also promote the formation of methane, which is undesirable in the ETH reaction. In addition, the presence of Fe^{3+} species can also promote coke formation *via* a mechanism involving the dehydrogenation of ethylene to form ethyl radicals, followed by the addition of ethyl radicals to form higher hydrocarbons and coke. The formation of coke can lead to the deactivation of the catalyst and the loss of activity and selectivity towards the desired hydrocarbon products.[16]

Furthermore, the appreciable performance of the novel catalyst used in this study can also be attributed to the low Si/Al.[40] Costa, Uguina[52] established that the production of liquid HCs is more favourable on HZSM-5 zeolites with low Si/Al ratios. In a separate investigation, Talukdar, Bhattacharyya[53] studied the conversion of a 50% ethanol aqueous solution using two ZSM-5 catalysts with Si/Al of 20 and 103. The zeolite with a Si/Al of 20 exhibited superior yields in liquid HCs, whereas the catalyst with a higher ratio (103) predominantly favoured light molecular weight (C_2–C_4) HCs. This demonstrates the suitability of zeolite catalysts with lower Si/Al ratios and increased acidity for converting ethanol into C_5^+ HCs. In recent research,[54] ZSM-5 catalysts with different Si/Al (16 to 500) were evaluated for their potential for ETH conversion. The catalyst with low Si/Al (<50) demonstrated significant stability and product selectivity towards heavier molecular (C_5^+) HCs, indicating an equilibrium between the Brønsted acid sites and radicals on the active catalysts.

3.2. Analysis of spent catalysts

3.2.1. Catalyst coking and deactivation – TGA-DTA study. The deposition of coke on spent catalysts after LATH (T = 350 °C and WHSV = 7 h^{-1}) was investigated using TGA-DTA. The calculation of coke deposition excluded the weight loss in the temperature range of 0–200 °C, which mainly corresponds to the removal of absorbed water and volatile compounds. Weight loss between 200–400 °C and 400–600 °C was attributed to the combustion of soft and hard coke, respectively, while weight loss between 600–800 °C indicated the removal of non-volatile and heavy compounds attached to the catalyst after the reaction.[55] The pure sample, denoted as HZSM-5 (pure), served as a reference and showed the lowest weight loss (at 200–800 °C) among all the processes, as it did not undergo HC reaction and had no coke deposition. In the MTH process, Fe/HZSM-5 exhibited the lowest deposition of soft coke, with a weight loss of 0.99 wt% among the spent catalysts, followed by the Ni and Co-doped catalysts, while the unmodified catalysts showed the highest soft coke deposit (1.70 wt%) (Fig. 6(a)). This showed the ability of metal species to impede the formation of coke. Ni/HZSM-5 demonstrated exceptional stability with the least coke deposition (3.33 wt%) between 400–600 °C, whereas Co/HZSM-5 exhibited the highest weight loss (6.32 wt%) due to increased deposition of hard coke, making it prone to deactivation. The accumulation of non-volatile compounds was more evident in the Ni-doped catalyst, resulting in the highest weight loss (2.10 wt%) compared to other spent catalysts. The trend of weight loss due to the burning of coke deposits (200–600 °C)

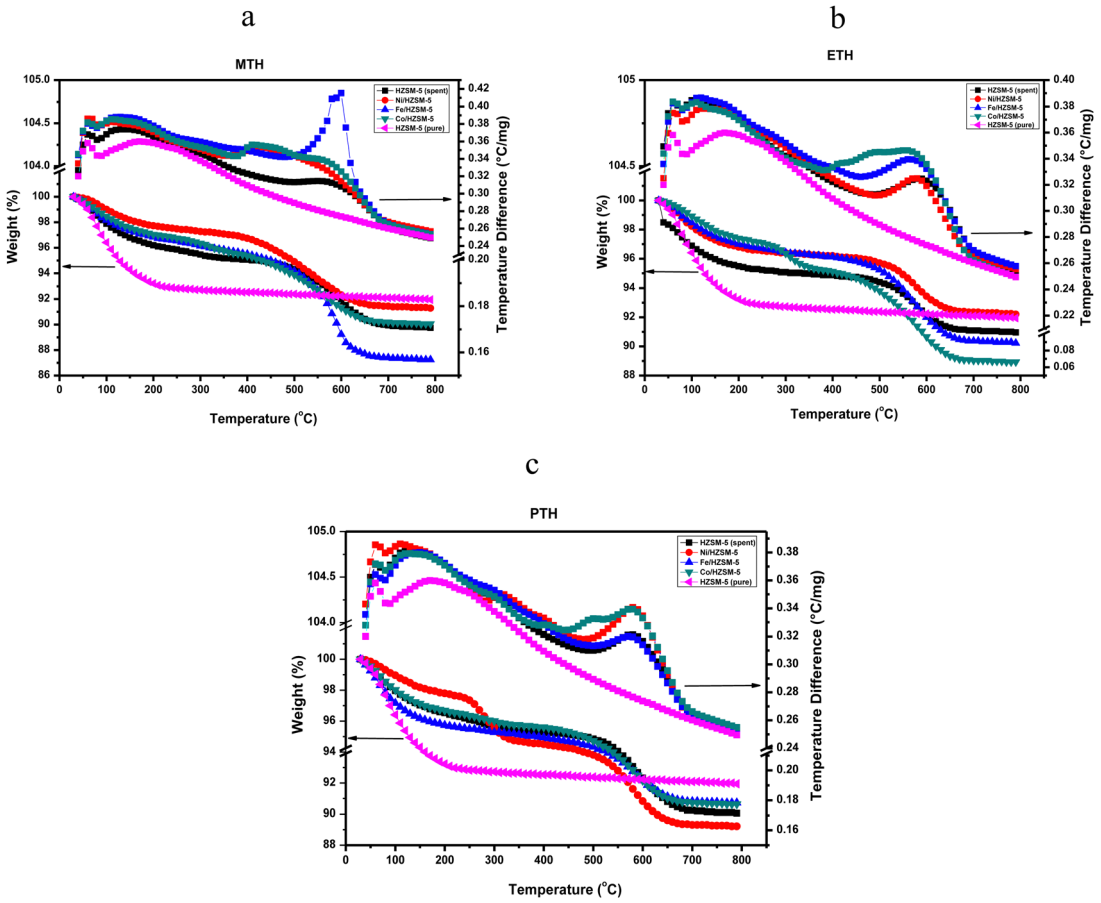

Fig. 6 TGA-DTA profile of (a) MTH, (b) ETH and (c) PTH conversion at T = 350 °C and WHSV = 7 h^{-1}.

followed the order: Ni/HZSM-5 < Fe/HZSM-5 < HZSM-5 < Co/HZSM-5.

Similar to MTH, Ni/HZSM-5 exhibited significant stability with the least weight reduction at 200–400 °C (0.61 wt%) and 400–600 °C (2.82 wt%) among the spent catalysts in ETH conversion (Fig. 6(b)). The unmodified catalyst also demonstrated comparable stability, accounting for 0.70 and 3.10 wt% weight loss from the combustion of soft and hard coke, while the Co-doped catalyst exhibited the least stability and a higher tendency for deactivation, with weight losses of 2.20 and 4.54 wt% respectively. However, compared to other catalysts, the unmodified catalyst (HZSM-5) showed the highest accumulation of non-volatile and heavy compounds, resulting in a significant decrease in catalyst weight (3.34 wt%) at 600–800 °C, while other catalysts recorded weight losses ranging from 1.20 to 1.81 wt%. The trend of weight loss due to the burning of coke deposits in the ETH process followed the pattern: Ni/HZSM-5 < HZSM-5 < Fe/HZSM-5 < Co/HZSM-5, with weight losses of 3.35, 3.80, 5.01, and 6.74 wt% respectively. Interestingly, Co/HZSM-5 exhibited the lowest weight loss (with 0.8 and 2.8 wt% attributed to the burning of soft and hard coke and 1.4 wt% due to the removal of non-volatile compounds) in the PTH conversion as opposed to MTH and ETH (Fig. 6(c)). Fe/HZSM-5 displayed the least stability in the PTH process, with coke deposition accounting for 3.30 and 3.71 wt% respectively. The trend of coke deposition in the PTH process followed the order: Co/HZSM-5 < Ni/HZSM-5 < HZSM-5 < Fe/HZSM-5, *i.e.*, 3.57, 4.21, 4.54, 6.96 wt% weight loss respectively. Due to the presence of an additional carbon atom in propanol compared to ethanol, it exhibits higher susceptibility to carbon–carbon bond cleavage reactions. As a result, more reactive intermediates are formed, which can further polymerize into coke precursors. This explains the increased deposition of coke in the PTH process.

The discrepancies in stability and coke deposition of different catalysts examined can be attributed to different factors. It is important to note that coke deposition in zeolite catalysts is a complex phenomenon influenced by multiple factors that can interact. Experimental conditions, such as temperature, space velocity, metal type, catalyst properties, feedstock type, and reaction pathway and kinetics, including the rate of dehydrogenation and subsequent reactions, can play a role in determining coke deposition. Contrary to MTH and ETH, the lowest coke deposition exhibited by Co/HZSM-5 in PTH was suggested to be due to different molecular structures and properties of the low alcohol feedstock. Among the catalysts investigated for coke deposition from the LATH conversion, Ni/HZMS-5 exhibited the highest stability with the lowest cumulative coke

Table 2 Comparative evaluation of average weight loss (wt%) of spent catalysts at T = 350 °C and WHSV = 7 h^{-1}

Temperature	Ni/HZSM-5	Fe/HZSM-5	Co/HZSM-5	HZSM-5 (spent)	HZSM-5 (pure)
MTH					
0–200 (W + V)	3.80	2.28	3.16	2.96	6.78
200–600 (S + H)	4.39	5.39	7.61	5.71	0.98
200–800 (SH + NV)	6.46	6.43	9.58	7.00	1.28
ETH					
0–200 (W + V)	3.21	2.99	2.61	2.57	6.78
200–600 (S + H)	3.35	5.01	6.74	3.80	0.98
200–800 (SH + NV)	4.59	6.77	8.46	7.05	1.28
PTH					
0–200 (W + V)	9.95	10.79	9.28	9.37	8.06
200–600 (S + H)	4.21	6.96	3.57	4.54	0.98
200–800 (SH + NV)	6.48	8.58	5.01	6.07	1.28

Weight loss due to W + V – absorbed H_2O & volatiles; S + H – soft and hard coke; NV – non-volatiles.

deposition (12.01 wt%), followed by HZSM-5 (14.10 wt%), Fe/HZSM-5 (17.42 wt%) and finally Co/HZSM-5 which recorded the highest cumulative weight loss at 17.91 wt%. The significant stability exhibited by the incorporation of Ni into the zeolite framework can be due to strong metal-support interactions, which enhance the stability of the catalyst. This suggests that the presence of active metals, in some cases, can suppress coke formation and promote the cracking of coke precursors to enhance the formation of desired products. Other studies have reported a similar trend.[56,57] The weight loss observed in the thermogravimetric analysis (TGA) pattern corresponds to the differential thermal analysis (DTA) profile in Fig. 6(a)–(c). Notably, the DTA peaks associated with coke combustion align with the weight loss observed in the TGA patterns. This correlation indicates the tendency of coke deposition and subsequent catalyst deactivation in the examined spent catalysts. Table 2 presents the average weight loss of spent catalysts after LATH conversion.

According to reports by Chen, Grønvold.[58] and Guisnet,[59] the retention of organic species within the ZSM-5 zeolite plays a crucial role in the LATH process. Initially, these organic species act as active sites, but as the process progresses, they inhibit catalytic activity. During the induction phase, the proposed mechanism is based on the hydrocarbon pool model, which suggests that the active sites in the zeolite are hybrid organic–inorganic structures consisting of cyclic organic species within the zeolite framework. Interestingly, the yields of olefins and aromatics do not remain high during the initial reaction. Olsbye, Bjørgen[60] investigated the retained material in catalysts such as H-beta zeolite, SAPO-34, and H-ZSM-5 after conversion. They found that the development of the hydrocarbon pool involves the breakdown of reactants, and once the pool is formed, the olefins and aromatics desorb from the catalysts. However, the active organic species can transform into larger aromatic molecules, depositing in the catalyst's pores and surface, which leads to pore blockage and decreased catalytic performance. At low temperatures, carbonaceous deposits known as soft coke mainly consist of oligomers and polymers derived from the reactant through condensation and rearrangement processes. In contrast, high-temperature coke or coke formed over a prolonged time-on-stream is primarily composed of polyaromatics (hard coke), requiring not only condensation and rearrangement steps but also various hydrogen-transfer and dehydrogenation steps on acidic catalysts.[61]

The presence of active metals can affect the production and distribution of coke deposits on the catalyst's surface and the coke deposits' nature and content. Metal-loading of the catalyst greatly increases the amount of coke production, which can be attributed to an increased concentration of total acid sites compared to HZSM-5. However, Ni-doped displayed appreciably greater stability than HZSM-5 catalysts. It is possible to ascribe the amount of coke that is created on the catalyst to be dependent on the strength of the acid sites and the type of metal impregnated on the catalyst. Co/HZSM-5 and Fe/HZSM-5 are two examples of catalysts that display the most severe coking, which suggests a short lifetime in continuous operations. The addition of metals, on the other hand, speeds up the combustion of coke. According to the findings of the TGA, the temperature at which the catalyst is regenerated falls within the range of 500–600 °C. Further on, the temperature required for regeneration may end up being lower for metal-loaded catalysts. This can be attributed to the catalytic effect that impregnated metals have on burning carbonaceous materials.[62] A lower catalyst regeneration temperature reduces strain on the catalyst, potentially leading to an extended lifetime in industrial applications.[63,64] Nevertheless, further research is required to validate this hypothesis.

3.2.2. Structural and morphological properties of spent catalysts from ETH. The XRD analysis of spent HZSM-5, Ni/HZSM-5, Fe/HZSM-5, and Co/HZSM-5 catalysts after ETH conversion provided valuable information about the structural changes in the catalyst after the catalytic reaction. The XRD patterns of spent catalysts show a decrease in the intensity of diffraction peaks, which is more prominent in Co/HZSM-5 catalyst due to the catalytic reaction and the accumulation of coke deposits (Fig. 7(a)). The intensity reduction is more pronounced in the (101) and (200) planes, which are the most sensitive to structural changes. In addition, the XRD pattern

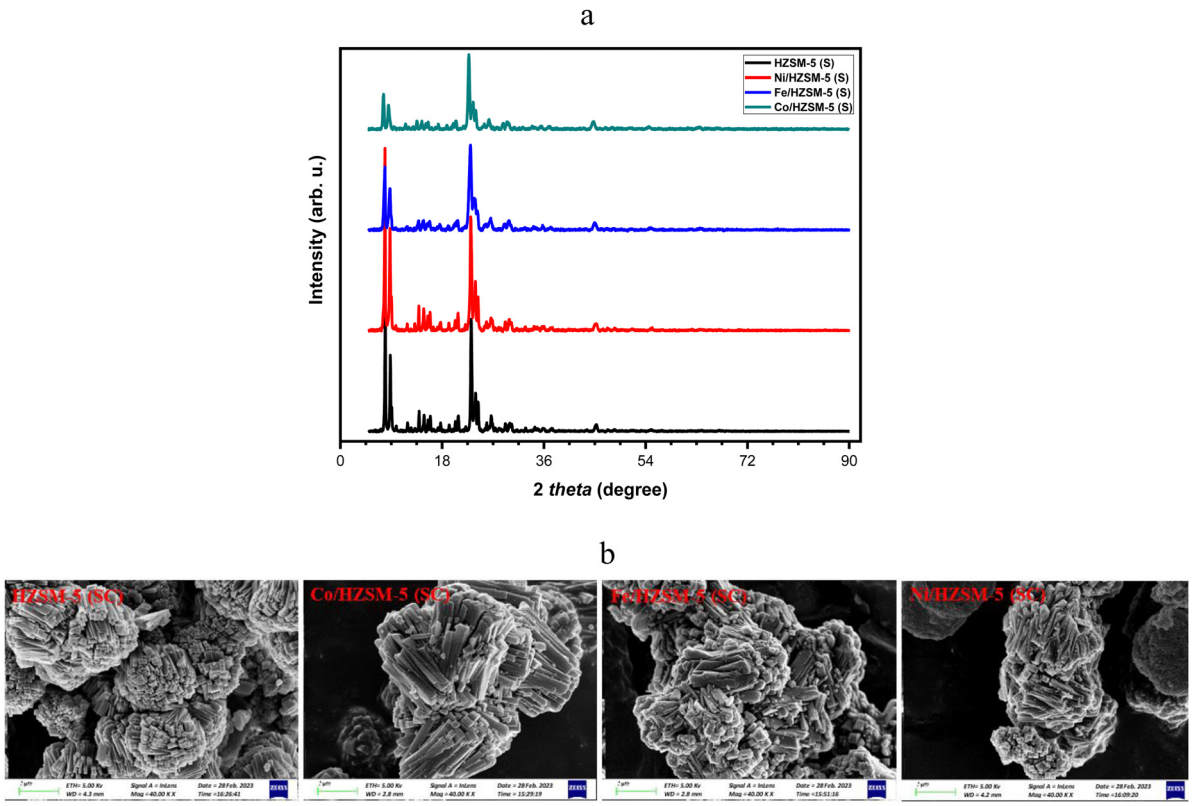

Fig. 7 (a) XRD pattern and (b) SEM images of spent catalysts (operating condition: 350 °C and 7 h^{-1}).

also revealed that the MFI zeolite framework was retained after the catalytic process, irrespective of the carbon deposition. The extent of framework collapse is less pronounced in the Ni-doped catalysts than in other catalysts. This suggests that active Ni metal can stabilise the zeolite structure and somewhat mitigate framework collapse. Nevertheless, the substantial decrease in the characteristic peak (7–9°) of the Co/HZSM-5 catalyst corresponds to an increased coke deposit on the catalyst. This observation aligns with the TGA-DTA results, which indicate that Ni/HZSM-5 and Co/HZSM-5 exhibited the lowest and highest coke deposition after the ETH conversion. The SEM images of spent catalysts typically show surface features such as aggregates of small crystals to form microspheres (Fig. 7(b)), similar to the original catalyst. The SEM images can also partly observe coke deposits on the catalyst surface as dark regions. The presence of active metals can influence the formation and distribution of coke deposits on the catalyst surface, which may affect the modified catalyst's surface features.

The FTIR spectra of spent catalysts typically show the presence of various functional groups and species, including adsorbed water, silanol groups, and coke deposits (Fig. 8(a) and (b)). The FTIR result showed that the functional groups of the spent catalyst were preserved despite the coke deposition after the

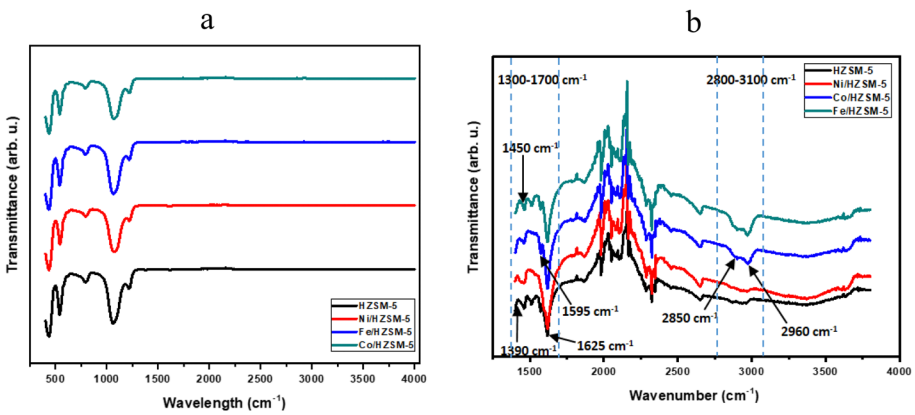

Fig. 8 FTIR spectra (a) 400–4000 cm^{-1} (b) 1300–3800 cm^{-1}.

LATH conversion. FTIR spectroscopy was used to identify the bond vibrations of the catalyst and adsorbed HCs on spent catalysts after the LATH conversion. The presence of coke can be detected by the characteristic bands of HC molecules. The key regions in the FTIR spectrum for coke characterization are 1300–1700 cm^{-1} and 2800–3100 cm^{-1}. Fig. 8(b) depicts the spectra of spent catalysts within these regions (1300–3800 cm^{-1}). The vibrations in the first range (1300–1700 cm^{-1}) are associated with polycondensed aromatics, conjugated olefins, and some aliphatic bending modes, while the vibrations in the second range (2800–3100 cm^{-1}) correspond to aliphatics (asymmetric and symmetric stretching) and single-ring aromatics. To analyse each vibration, the spectra of the spent catalysts were identified by individual peaks:[65–68] 1390 cm^{-1}, terminal $-CH_3$ groups; 1450 cm^{-1}, combination of aliphatics and alkyl aromatics; 1595 cm^{-1}, coke band or polycondensed aromatics; 1620 cm^{-1}, double bonds or olefins; 2850 cm^{-1}, $-CH_2$ groups; 2960 cm^{-1}, $-CH_3$ groups. It is important to note that these numbers are estimates and may have some discrepancies due to some factors. Compared to the unmodified catalyst, the most abundant band seen more clearly in the Fe- and Co-doped HZSM-5 in the 2800–3100 cm^{-1} range corresponds to the CH_2 (2850 cm^{-1}) and $-CH_3$ (2960 cm^{-1}) groups, indicating the presence of long or naphthenic aliphatic chains in the coke produced on the catalyst. In this region, a higher concentration of CH_3 groups than CH_2 groups was observed in the coke, following the order Fe/HZSM-5 Co/HZSM-5 > Ni/HZSM-5 > HZSM-5.

However, the band in this range (2800–3100 cm^{-1}) exhibits lower intensity, indicating that the coke is predominately unsaturated. In addition, the most abundant band in the 1300–1700 cm^{-1} range at 1625 cm^{-1} is more pronounced in the metal-doped samples than in the unmodified catalysts. This indicates that more double-bonded or olefinic HCs are formed with the metal-doped catalyst than unmodified ones. The findings of this study are consistent with those of previous studies.[65,66,68] It can be suggested that the presence of metal species shifted and facilitated coke composition towards olefin HCs and long aliphatic chains, attributed to further secondary reactions, including aromatization and oligomerization favoured by these metal species. The reaction products and adsorbed HC trends discussed and shown in Fig. 1–3 are consistent with typical expectations for the LATH conversion reaction.[68–70] These trends showed the production of olefins, which correlates directly with the extent of conversion, indicating their role as reaction intermediates, while the formation of heavy aliphatic and aromatics represent the final products.[70] These results are consistent with the overall mechanism of the LATH reaction.

4. Conclusion

The catalytic performance of transition metal-doped catalysts in low alcohol to hydrocarbon (LATH) conversion was investigated under different conditions, with temperatures of 350 and 400 °C and WHSV of 7 and 12 h^{-1}. Catalyst characterisation using different techniques showed the successful incorporation of transition metals (Ni, Fe and Co) into ZSM-5 zeolite catalyst.

Evaluation of these catalysts in LATH conversion revealed their activity on various low alcohol feedstocks, with all catalysts showing >97% conversion of low alcohol and considerable preference for C_5–C_8 HCs (30–70% selectivity). In particular, Co/HZSM-5 showed considerable selectivity for BTX (11.0%) compared to other catalysts, while Ni/HZSM-5 favoured the production of C_{12}^+ (7.40%) and C_9–C_{12} (2.91%) in MTH. The product selectivity for ETH and PTH exhibits a close correlation. In addition, Ni/HZSM-5 showed the highest selectivity towards C_9–C_{12} (24.4%), while Fe/HZSM-5 and HZSM-5 improved the synthesis of BTX (6.01%) and C_{12}^+ (39.42%) HCs, respectively, in the ETH process. However, in PTH conversion, Ni/HZSM-5 exhibited greater selectivity for C_{12}^+ (36.51%) and BTX (10.71%), while Co/HZSM-5 and Fe/HZSM-5 improved the synthesis of C_5–C_8 (63.92%) and C_9–C_{12} (9.62%), respectively. The increase in WHSV and temperature favoured the production of liquid hydrocarbons (C_5^+), with a specific increase in C_5–C_8 HCs observed in the LATH process. The catalytic process showed that the modified catalysts improved the selectivity for liquid hydrocarbons and outperformed the unmodified catalysts in the LATH conversion, which exhibited appreciable selectivity for C_{12}^+ products only in the ETH process.

The coke deposition study provided important insight into the coke deposition on spent catalysts during LATH conversion. The TGA-DTA study showed that Ni/HZSM-5 exhibited excellent stability with the least coke deposition, while Co/HZSM-5 had a higher tendency to coke deposition and deactivation, resulting in significant weight loss (9.60 and 8.51 wt%) in MTH and ETH conversion. In the PTH process, Co/HZSM-5 showed the lowest weight loss (5.0 wt%), and Fe/HZSM-5 exhibited the lowest stability. Among the catalysts tested, the Ni/HZSM catalyst exhibited remarkable stability and catalytic performance in LATH conversion. Structural evaluation of the spent catalysts revealed that they maintained their characteristic framework throughout the LATH conversion process despite coke deposition. These results are important for understanding the selectivity and behaviour of different catalysts during LATH conversion and provide valuable insights for optimising catalyst selection and operating conditions to minimise coke deposition and maximise catalyst stability. These results not only contribute to a better understanding of LATH conversion processes but also have significant implications for exploring strategies to reduce coke formation and improve the overall efficiency of single-step LATH conversion. This study contributes to the advancement and development of more efficient catalysts for the conversion of low alcohol to fuel-range hydrocarbons.

Conflicts of interest

There are no conflicts to declare.

Acknowledgements

This work is financially supported by an international collaborative project (BRICS2019-040) under the BRICS STI Framework Programme with government funding organisations of South Africa NRF (BRIC190321424123), Brazil CNPq (402849/2019-1), Russia RFBR (19-58-80016), India DST (CRG/2018/004610, DST/TDT/TDP-011/2017) and China MOST (2018YFE0183600).

References

1 A. B. Stambouli, Z. Khiat, S. Flazi and Y. Kitamura, A review on the renewable energy development in Algeria: Current perspective, energy scenario and sustainability issues, *Renewable Sustainable Energy Rev.*, 2012, **16**(7), 4445–4460.
2 I. M. S. Anekwe and Y. M. Isa, Catalytic Conversion of Low Alcohol to Hydrocarbons: Challenges, Prospects, and Future Work Considerations, *Int. J. Energy Res.*, 2023, **2023**, 1648449.
3 G. Carotenuto, R. Tesser, M. Di Serio and E. Santacesaria, Bioethanol as feedstock for chemicals such as acetaldehyde, ethyl acetate and pure hydrogen, *Biomass Convers. Biorefin.*, 2013, **3**(1), 55–67.
4 J. Han, L. M. T. Somers, R. Cracknell, A. Joedicke, R. Wardle and V. R. R. Mohan, Experimental investigation of ethanol/diesel dual-fuel combustion in a heavy-duty diesel engine, *Fuel*, 2020, **275**, 117867.
5 J. Zhu, S. Wang, M. Raza, Y. Feng, J. Li and Y. Mao, *et al.*, Autoignition behavior of methanol/diesel mixtures: Experiments and kinetic modeling, *Combust. Flame*, 2021, **228**, 1–12.
6 H. Y. Kim, J. C. Ge and N. J. Choi, Effects of Ethanol–Diesel on the Combustion and Emissions from a Diesel Engine at a Low Idle Speed, *Appl. Sci.*, 2020, **10**(12), 4153.
7 K. Van der Borght, V. V. Galvita and G. B. Marin, Ethanol to higher hydrocarbons over Ni, Ga, Fe-modified ZSM-5: Effect of metal content, *Appl. Catal., A*, 2015, **492**, 117–126.
8 N. Rahimi and R. Karimzadeh, Catalytic cracking of hydrocarbons over modified ZSM-5 zeolites to produce light olefins: A review, *Appl. Catal., A*, 2011, **398**(1–2), 1–17.
9 M. Juybar, M. Kanmohammadi Khorrami and A. Bagheri Garmarudi, Conversion of methanol to aromatics over ZSM-5/11 intergrowth Zeolites and bimetallic Zn–Cu-ZSM-5/11 and Ga-Ag-ZSM-5/11 catalysts prepared with direct synthesis method, *J. Chem. Sci.*, 2019, **131**(10), 104.
10 C. D. Chang and A. J. Silvestri, The conversion of methanol and other O-compounds to hydrocarbons over zeolite catalysts, *J. Catal.*, 1977, **47**(2), 249–259.
11 K. K. Ramasamy, H. Zhang, J. Sun and Y. Wang, Conversion of ethanol to hydrocarbons on hierarchical HZSM-5 zeolites, *Catal. Today*, 2014, **238**, 103–110.
12 C. K. Narula, Z. Li, E. M. Casbeer, R. A. Geiger, M. Moses-Debusk and M. Keller, *et al.*, Heterobimetallic zeolite, InV-ZSM-5, enables efficient conversion of biomass derived ethanol to renewable hydrocarbons, *Sci. Rep.*, 2015, **5**(1), 16039.
13 R. Le Van Mao, P. Levesque, G. McLaughlin and L. Dao, Ethylene from ethanol over zeolite catalysts, *Appl. Catal.*, 1987, **34**, 163–179.
14 R. Le Van Mao, T. M. Nguyen and G. P. McLaughlin, The bioethanol-to-ethylene (BETE) process, *Appl. Catal.*, 1989, **48**(2), 265–277.
15 C. B. Phillips and R. Datta, Production of Ethylene from Hydrous Ethanol on H-ZSM-5 under Mild Conditions, *Ind. Eng. Chem. Res.*, 1997, **36**(11), 4466–4475.
16 J. Sun and Y. Wang, Recent advances in catalytic conversion of ethanol to chemicals, *ACS Catal.*, 2014, **4**(4), 1078–1090.
17 T. Zaki, Catalytic dehydration of ethanol using transition metal oxide catalysts, *J. Colloid Interface Sci.*, 2005, **284**(2), 606–613.
18 T. Nguyen and R. Le Van Mao, Conversion of ethanol in aqueous solution over ZSM-5 zeolites: Study of the reaction network, *Appl. Catal.*, 1990, **58**(1), 119–129.
19 L. Qi, Y. Wei, L. Xu and Z. Liu, Reaction behaviors and kinetics during induction period of methanol conversion on HZSM-5 zeolite, *ACS Catal.*, 2015, **5**(7), 3973–3982.
20 Y. Zhi, H. Shi, L. Mu, Y. Liu, D. Mei and D. M. Camaioni, *et al.*, Dehydration Pathways of 1-Propanol on HZSM-5 in the Presence and Absence of Water, *J. Am. Chem. Soc.*, 2015, **137**(50), 15781–15794.
21 A. T. Aguayo, D. Mier, A. G. Gayubo, M. Gamero and J. Bilbao, Kinetics of methanol transformation into hydrocarbons on a HZSM-5 zeolite catalyst at high temperature (400–550 °C), *Ind. Eng. Chem. Res.*, 2010, **49**(24), 12371–12378.
22 R. Liu, X. Shao, C. Wang, W. Dai and N. Guan, Reaction mechanism of methanol-to-hydrocarbons conversion: Fundamental and application, *Chin. J. Catal.*, 2023, **47**, 67–92.
23 K. Van der Borght, R. Batchu, V. V. Galvita, K. Alexopoulos, M. F. Reyniers and J. W. Thybaut, *et al.*, Insights into the Reaction Mechanism of Ethanol Conversion into Hydrocarbons on H-ZSM-5, *Angew. Chem., Int. Ed.*, 2016, **55**(41), 12817–12821.
24 E. G. Derouane, J. B. Nagy, P. Dejaifve, J. H. C. van Hooff, B. P. Spekman and J. C. Védrine, *et al.*, Elucidation of the mechanism of conversion of methanol and ethanol to hydrocarbons on a new type of synthetic zeolite, *J. Catal.*, 1978, **53**(1), 40–55.
25 P. Tynjälä, T. T. Pakkanen and S. Mustamäki, Modification of ZSM-5 Zeolite with Trimethyl Phosphite. 2. Catalytic Properties in the Conversion of C1–C4 Alcohols. The, *J. Phys. Chem. B*, 1998, **102**(27), 5280–5286.
26 P. Tynjälä, T. T. Pakkanen and S. Mustamäki, Modification of ZSM-5 Zeolite with Trimethyl Phosphite. 2. Catalytic Properties in the Conversion of C1–C4 Alcohols. The, *J. Phys. Chem. B*, 1998, **102**(27), 5280–5286.
27 U. Dwivedi, K. K. Pant and S. N. Naik, Controlling liquid hydrocarbon composition in valorization of plastic waste *via* tuning zeolite framework and SiO_2/Al_2O_3 ratio, *J. Environ. Manage.*, 2021, **297**, 113288.
28 G. Ramya, R. Sudhakar, J. A. I. Joice, R. Ramakrishnan and T. Sivakumar, Liquid hydrocarbon fuels from jatropha oil

through catalytic cracking technology using AlMCM-41/ZSM-5 composite catalysts, *Appl. Catal., A*, 2012, **433–434**, 170–178.

29 Q. Li, F. Zhang, J. Jarvis, P. He, M. M. Yung and A. Wang, *et al.*, Investigation on the light alkanes aromatization over Zn and Ga modified HZSM-5 catalysts in the presence of methane, *Fuel*, 2018, **219**, 331–339.

30 Y. Bi, Y. Wang, X. Chen, Z. Yu and L. Xu, Methanol aromatization over HZSM-5 catalysts modified with different zinc salts, *Chin. J. Catal.*, 2014, **35**(10), 1740–1751.

31 J. Kim, M. Choi and R. Ryoo, Effect of mesoporosity against the deactivation of MFI zeolite catalyst during the methanol-to-hydrocarbon conversion process, *J. Catal.*, 2010, **269**(1), 219–228.

32 I. M. S. Anekwe, B. Oboirien and Y. M. Isa, Catalytic conversion of bioethanol over cobalt and nickel-doped HZSM-5 zeolite catalysts, *Biofuels, Bioprod. Biorefin.*, 2023, 686–700.

33 Y. Sun, T. Ma, L. Zhang, Y. Song, Y. Shang and Y. Zhai, *et al.*, The influence of zoned Al distribution of ZSM-5 zeolite on the reactivity of hexane cracking. Molecular, *Catalysis*, 2020, **484**, 110770.

34 D. P. Gamliel, G. M. Bollas and J. A. Valla, Bifunctional Ni-ZSM-5 Catalysts for the Pyrolysis and Hydropyrolysis of Biomass, *Energy Technol.*, 2017, **5**(1), 172–182.

35 Y. Tang, D. Dubbeldam and S. Tanase, Water-Ethanol and Methanol-Ethanol Separations Using in Situ Confined Polymer Chains in a Metal-Organic Framework, *ACS Appl. Mater. Interfaces*, 2019, **11**(44), 41383–41393.

36 Z. Song, H. Huang, W. Xu, L. Wang, Y. Bao and S. Li, *et al.*, Continuously Adjustable, Molecular-Sieving ''Gate'' on 5A Zeolite for Distinguishing Small Organic Molecules by Size, *Sci. Rep.*, 2015, **5**, 13981.

37 A. Hamins and K. Seshadri, The influence of alcohols on the combustion of hydrocarbon fuels in diffusion flames, *Combust. Flame*, 1986, **64**(1), 43–54.

38 C. Lamy, E. Belgsir and J. Leger, Electrocatalytic oxidation of aliphatic alcohols: Application to the direct alcohol fuel cell (DAFC), *J. Appl. Electrochem.*, 2001, **31**, 799–809.

39 W. Zhou, B. Zhou, W. Li, Z. Zhou, S. Song and G. Sun, *et al.*, Performance comparison of low-temperature direct alcohol fuel cells with different anode catalysts, *J. Power Sources*, 2004, **126**(1–2), 16–22.

40 A. G. Gayubo, A. M. Tarrío, A. T. Aguayo, M. Olazar and J. Bilbao, Kinetic modelling of the transformation of aqueous ethanol into hydrocarbons on a HZSM-5 zeolite, *Ind. Eng. Chem. Res.*, 2001, **40**(16), 3467–3474.

41 A. T. Aguayo, A. G. Gayubo, A. Atutxa, M. Olazar and J. Bilbao, Catalyst deactivation by coke in the transformation of aqueous ethanol into hydrocarbons. Kinetic modeling and acidity deterioration of the catalyst, *Ind. Eng. Chem. Res.*, 2002, **41**(17), 4216–4224.

42 A. G. Gayubo, A. Alonso, B. Valle, A. T. Aguayo, M. Olazar and J. Bilbao, Hydrothermal stability of HZSM-5 catalysts modified with Ni for the transformation of bioethanol into hydrocarbons, *Fuel*, 2010, **89**(11), 3365–3372.

43 A. G. Gayubo, A. Alonso, B. Valle, A. T. Aguayo, M. Olazar and J. Bilbao, Kinetic modelling for the transformation of bioethanol into olefins on a hydrothermally stable Ni–HZSM-5 catalyst considering the deactivation by coke, *Chem. Eng. J.*, 2011, **167**(1), 262–277.

44 C. D. Chang, MTG revisited, *Studies in Surface Science and Catalysis*, Elsevier, 1991, vol. 61, pp. 393–404.

45 W. Dongliang, X. Su, Z. Fan, Z. Wen, N. Li and Y. Yang, Recent Advances for Selective Catalysis in Benzene Methylation: Reactions, Shape-Selectivity and Perspectives, *Catal. Surv. Asia*, 2021, **25**, 1–15.

46 K. Tanabe, *Solid acids and bases: their catalytic properties*, Elsevier, 2012.

47 K. K. Ramasamy and Y. Wang, Ethanol conversion to hydrocarbons on HZSM-5: Effect of reaction conditions and Si/Al ratio on the product distributions, *Catal. Today*, 2014, **237**, 89–99.

48 P. Iadrat and C. Wattanakit, Bioethanol Upgrading to Renewable Monomers Using Hierarchical Zeolites: Catalyst Preparation, Characterization, and Catalytic Studies, *Catalysts*, 2021, **11**(10), 1162.

49 J. H. Kwak, R. Rousseau, D. Mei, C. H. F. Peden and J. Szanyi, The Origin of Regioselectivity in 2-Butanol Dehydration on Solid Acid Catalysts, *ChemCatChem*, 2011, **3**(10), 1557–1561.

50 S. Roy, G. Mpourmpakis, D.-Y. Hong, D. G. Vlachos, A. Bhan and R. J. Gorte, Mechanistic Study of Alcohol Dehydration on γ-Al_2O_3. ACS, *Catalysis*, 2012, **2**(9), 1846–1853.

51 M. J. Janik, J. Macht, E. Iglesia and M. Neurock, Correlating acid properties and catalytic function: a first-principles analysis of alcohol dehydration pathways on polyoxometalates, *J. Phys. Chem. C*, 2009, **113**(5), 1872–1885.

52 E. Costa, A. Uguina, J. Aguado and P. J. Hernandez, Ethanol to gasoline process: effect of variables, mechanism, and kinetics, *Ind. Eng. Chem. Process Des. Dev.*, 1985, **24**(2), 239–244.

53 A. K. Talukdar, K. G. Bhattacharyya and S. Sivasanker, HZSM-5 catalysed conversion of aqueous ethanol to hydrocarbons, *Appl. Catal., A*, 1997, **148**(2), 357–371.

54 F. F. Madeira, K. B. Tayeb, L. Pinard, H. Vezin, S. Maury and N. Cadran, Ethanol transformation into hydrocarbons on ZSM-5 zeolites: Influence of Si/Al ratio on catalytic performances and deactivation rate. Study of the radical species role, *Appl. Catal., A*, 2012, **443**, 171–180.

55 R. Ahmed, C. Sinnathamb and D. Subbarao, Kinetics of decoking of spent reforming catalyst, *J. Appl. Sci.*, 2011, **11**(7), 1225–1230.

56 H. Persson, I. Duman, S. Wang, L. Pettersson and W. Yang, Catalytic pyrolysis over transition metal-modified zeolites: A comparative study between catalyst activity and deactivation, *J. Anal. Appl. Pyrolysis*, 2019, **138**, 54–61.

57 J. Su, Y. Liu, W. Yao and Z. Wu, Catalytic combustion of dichloromethane over HZSM-5-supported typical transition metal (Cr, Fe, and Cu) oxide catalysts: a stability study, *J. Phys. Chem. C*, 2016, **120**(32), 18046–18054.

58 D. Chen, A. Grønvold, K. Moljord and A. Holmen, Methanol conversion to light olefins over SAPO-34: reaction network

and deactivation kinetics, *Ind. Eng. Chem. Res.*, 2007, **46**(12), 4116–4123.

59 M. Guisnet, ''Coke'' molecules trapped in the micropores of zeolites as active species in hydrocarbon transformations, *J. Mol. Catal. A: Chem.*, 2002, **182**, 367–382.

60 U. Olsbye, M. Bjørgen, S. Svelle, K.-P. Lillerud and S. Kolboe, Mechanistic insight into the methanol-to-hydrocarbons reaction, *Catal. Today*, 2005, **106**(1–4), 108–111.

61 H. Zhang, S. Shao, R. Xiao, D. Shen and J. Zeng, Characterization of coke deposition in the catalytic fast pyrolysis of biomass derivates, *Energy Fuels*, 2014, **28**(1), 52–57.

62 P. B. Weisz and R. B. Goodwin, Combustion of carbonaceous deposits within porous catalyst particles: II. Intrinsic burning rate, *J. Catal.*, 1966, **6**(2), 227–236.

63 A. G. Gayubo, A. T. Aguayo, A. Atutxa, R. Prieto and J. Bilbao, Role of reaction-medium water on the acidity deterioration of a HZSM-5 zeolite, *Ind. Eng. Chem. Res.*, 2004, **43**(17), 5042–5048.

64 H. Persson, I. Duman, S. Wang, L. J. Pettersson and W. Yang, Catalytic pyrolysis over transition metal-modified zeolites: A comparative study between catalyst activity and deactivation, *J. Anal. Appl. Pyrolysis*, 2019, **138**, 54–61.

65 H. G. Karge, W. Nießen and H. Bludau, *In situ* FTIR measurements of diffusion in coking zeolite catalysts, *Appl. Catal., A*, 1996, **146**(2), 339–349.

66 L. Palumbo, F. Bonino, P. Beato, M. Bjørgen, A. Zecchina and S. Bordiga, Conversion of Methanol to Hydrocarbons: Spectroscopic Characterization of Carbonaceous Species Formed over H-ZSM-5. The, *J. Phys. Chem. C*, 2008, **112**(26), 9710–9716.

67 J. Robertson, Diamond-like amorphous carbon, *Mater. Sci. Eng., R*, 2002, **37**(4), 129–281.

68 J. Valecillos, H. Vicente, A. G. Gayubo, A. T. Aguayo and P. Castaño, Spectro-kinetics of the methanol to hydrocarbons reaction combining online product analysis with UV–vis and FTIR spectroscopies throughout the space time evolution, *J. Catal.*, 2022, **408**, 115–127.

69 J. Valecillos, E. Epelde, J. Albo, A. T. Aguayo, J. Bilbao and P. Castaño, Slowing down the deactivation of H-ZSM-5 zeolite catalyst in the methanol-to-olefin (MTO) reaction by P or Zn modifications, *Catal. Today*, 2020, **348**, 243–256.

70 S. Ilias and A. Bhan, Mechanism of the catalytic conversion of methanol to hydrocarbons, *ACS Catal.*, 2013, **3**(1), 18–31.